International Journal of Mineral Processing 114–117 (2012) 80–92

Contents lists available at SciVerse ScienceDirect

International Journal of Mineral Processing

journal homepage: www.elsevier.com/locate/ijminpro

Utilisation of ultrasonic treatment for upgrading of hematitic/goethitic iron ore fines

E. Donskoi [a,*], A.F. Collings [b,1], A. Poliakov [a], W.J. Bruckard [c]

[a] CSIRO Process Science and Engineering, PO Box 883, Kenmore, QLD 4069, Australia
[b] CSIRO Materials Science and Engineering
[c] CSIRO Process Science and Engineering, Box 312, Clayton South, VIC 3169, Australia

ARTICLE INFO

Article history:
Received 20 January 2012
Received in revised form 5 October 2012
Accepted 20 October 2012
Available online 30 October 2012

Keywords:
Iron ore fines
Ultrasound, ultrasonic
Beneficiation
Grade
Recovery

ABSTRACT

Ultrasonic waves in pulps containing iron ore fines can start, or significantly intensify, particle cleaning, de-agglomeration or disintegration. Some softer minerals, often gangue minerals with lower iron contents such as kaolinite or ochreous goethite, disintegrate several orders of magnitude faster than the valuable iron-bearing minerals such as magnetite or hematite. This facilitates selective disintegration of the gangue minerals leaving the valuable minerals mostly unchanged.

A set of experiments involving ultrasonic treatment of four Australian iron ore fine samples was undertaken using three different ultrasonic experimental setups. The effect of ultrasound duration, power and pulp density on the recoveries and grades of iron, alumina and silica was studied.

The results showed that for hematitic/goethitic ores, the application of ultrasound enabled soft material of relatively low iron grade to de-agglomerate from the larger size fractions and report to the ultrafine size fractions. Modelled de-sliming of the ultrasonically treated ores showed that de-sliming following ultrasonic treatment could significantly improve the product iron grade, while de-sliming with a finer cut size could also improve the iron recovery compared with de-sliming identical ore that had not been pre-treated with ultrasound. It has been shown mathematically that in some scenarios it may be possible to simultaneously increase the iron grade and iron recovery in the de-slimed product if the ore has been treated with ultrasound before de-sliming.

1. Introduction

It is well known that ultrasonic waves in water or a pulp can initiate, or significantly intensify, different physicochemical phenomena such as polymerisation and depolymerisation, emulsification and coagulation, surface cleaning, reduction and oxidation, activation, and even mineral disintegration. Vibrations in the water/pulp create a series of rarefactions and compressions and the nucleation of microbubbles can be initiated when there is a pressure drop within the rarefaction areas. There are two major mechanisms proposed for microbubble nucleation: liquid gasification, when the boiling point of the liquid is exceeded, and the release of dissolved gases (gaseous cavitations). The microbubbles collapse when their diameter exceeds a critical value, and such collapses can result in shock waves which can generate very localised high pressures (up to 5000 atm) and temperatures (up to 5000 K) (Ross, 1976; Mason and Lorimer, 1991; Gogate and Pandit, 2001; Didenko and Suslick, 2002; Flannigan and Suslick, 2005). These phenomena can significantly affect the physicochemical properties and reactions of liquid and solid phases in a pulp.

The utilisation of ultrasonic treatments to enhance the beneficiation of different minerals and coals has been extensively studied (Warren, 1992; Tao and Parekh, 2000; Farmer et al., 2000). It would seem reasonable to expect that ultrasonics may be useful in one or more of the different stages of iron ore beneficiation such as flotation, magnetic separation, or classification (hydrocycloning) to provide improvements in iron recovery and grade. Franko and Klima (2002) have reported that ultrasound treatment helps separate ultra fines attached to larger particles in iron ore beneficiation processes. In ground iron ores, these ultra fine size fractions generally have lower iron content and greater alumina and silica contents than the larger size fractions (Donskoi et al., 2008a, 2006a,b), thus providing opportunities for ore upgrading.

Donskoi et al. (2006b) have shown that application of ultrasound/stirring can have a significant effect on iron ore fines by liberating lower grade physically entrained ultrafines from larger size fractions, which increases the grade of the product after de-sliming. Later, utilising optical image analysis and automatic iron ore texture classification (Donskoi et al., 2010a, 2008b, 2007a), it has been shown (Donskoi et al., 2007b) that for the larger iron ore size fractions the mass proportion of textural classes containing higher amounts of ochreous goethite and kaolinite had significantly decreased after ultrasonic treatment. In contrast, the proportion of texture classes in which hematite and vitreous goethite were the major minerals had

* Corresponding author. Tel.: +61 7 3327 4158; fax: +61 7 3327 4682.
E-mail address: Eugene.Donskoi@csiro.au (E. Donskoi).
[1] Deceased.

0301-7516/$ – see front matter.
http://dx.doi.org/10.1016/j.minpro.2012.10.005

increased. The interpretation was (Donskoi et al., 2007b) that softer components of the ore, such as ochreous goethite, or aluminosilicate phases, such as kaolinite, significantly disintegrate when exposed to ultrasound treatment. Thus, it was shown that these two sub-processes of de-agglomeration and disintegration of the softer components of particles occurring during ultrasonic treatment could lead to improved product quality following hydrocyclone de-sliming. Pandey et al. (2010) also showed that ultrasound treatment followed by de-sliming could significantly reduce alumina, silica and phosphorous in two Indian iron ores. In their experiments, the optimal time of treatment was 5 min, after which the level of alumina and silica in the de-slimed product started increasing again. Their observation was explained by a so-called "fusion" effect. However, iron recovery data was not analysed, so there is also a strong possibility that after 5 min of treatment soft hematitic structures started to be disintegrated, which resulted in a decrease in the iron grade. The experiments by Pandey et al. (2010) were performed in an ultrasonic tank without stirring, and the treated ore settled on the bottom of the tank. The importance of ore suspension during sonication has not been shown. Our current research shows that the complete suspension of iron ore in the slurry can significantly improve the ultrasonic effect and can protect removed low grade material from "fusion" effects. The mineral composition of the ore was not discussed by Pandey et al. (2010), but our study (Donskoi et al., 2010b) shows that the ore composition is very important from the point of view of ultrasonic application. For example, our current research shows that the effect of ultrasound on magnetite ores with quartz is insignificant (Donskoi et al., 2010b). The other critical issues would seem to be the interdependence between product grade and iron recovery, the dependence of ultrasonic effects on the experimental setup, and the relationship between ore size distribution and iron grade. These aspects were not studied by Pandey et al. (2010).

In the present study, further test work has been conducted on a set of iron ore fine samples derived from Australian hematitic/goethitic ores. During the experiments, ultrasonic treatment was applied to the samples with the aim of investigating the effect of various experimental parameters on iron, alumina and silica product recovery and grade for different iron ores. In particular, different pulp density, ultrasonic duration, power, and contact method were considered. Size assay analysis of feed samples and products of ultrasound treatments was undertaken to see whether significant improvements in iron grade were possible after sonication and calculated classification (de-sliming), and to determine the interdependences between the recoveries and grades of iron, alumina and silica for the various ultrasonic treatments.

2. Experimental

Sonication experiments were performed on four different hematitic/goethitic iron ores using three different ultrasonic setups and applying ultrasonic treatments for different durations. Products from the experiments were sized, and the size fractions assayed, to compare the size and elemental distributions before and after the ultrasonic treatments. The data were analysed to calculate the iron grades and recoveries after modelled perfect cut de-sliming.

2.1. Head samples

Four different iron ore fine samples (Ores 1, 2, 3 and 4) were examined. All were derived from Australian hematitic/goethitic ores. The ore fine samples described in this article as Ore 1 and Ore 2 were fractions from two different ores with size below 300 μm. Size distributions for these samples are given later in the text. The ore fine samples described as Ore 3 and Ore 4 were derived from the same ore. Ore 3 was the −250 μm size fraction of the original sample and Ore 4 was the −2000 + 1000 μm size fraction of the same sample. Quantitative X-ray diffraction analysis (XRD) was conducted on selected ores and size fractions from some experimental products to determine the phases present. The XRD results for Ore 1 and Ore 3 are given in Table 1. The data show that the major minerals in these ores were hematite and goethite with some presence of kaolinite, gibbsite and quartz.

The majority of the results reported here relate to tests conducted on Ore 1. Results from tests on the other ores are given if they were principally different from the results for Ore 1, or where demonstration of repeatability for different ore types was required.

2.2. Setup 1 — circulating pulp

The first experimental setup (Setup 1) is shown in Fig. 1. An ultrasonic probe was introduced into a vertical glass retort partially filled with the iron ore pulp. The power yielded by the ultrasonic probe was ~150 W. A small pump provided recirculation of the pulp through the system at a rate of 2 l/min. The pulp flow was almost laminar, but strong enough to avoid particle settling.

The total volume of pulp was 120 ml, while the active volume, i.e. the volume of the retort where the iron ore slurry was exposed to ultrasound, was approximately 20 ml. As the iron ore fines were only exposed to ultrasound while in the retort, the actual time of ultrasonic treatment was approximately 6 times less than the total time of the experiment (i.e. for a 2 min experiment, the actual time of ultrasonic exposure was 20 s). For the majority of the experiments, the amount of ore used was 24 g and the volume of water was 114 ml giving a pulp density of ~17% solids. In one test (Exp 4), the pulp density was increased to 41% solids. Sonication times varied from 2 to 18 min. Details of the experimental conditions for the tests are given in Table 2.

During all experiments using this setup, significant heating of the pulp was observed. For example, at the end of Exp 1 (2 min sonication), the pulp temperature had risen from 24 °C to 39 °C, while at the end of Exp 3 (18 min sonication), the pulp temperature had reached 80 °C.

Experiments with ores with larger particle size (>500 μm) were not successful with this experimental setup — the large particles became stuck between the ultrasonic horn and the experimental retort preventing the pulp from circulating properly.

2.3. Setup 2 — tank setup

The second experimental setup (Setup 2) is shown in Fig. 2. Pulp was placed in the experimental vessel together with an impeller (for stirring) and an ultrasonic probe. Power delivered via the ultrasonic probe was reduced relative to Setup 1 (~110 W compared with ~150 W). The main reason for decreasing the power was the interference caused by the rotation of the impeller — coverage of the probe was not stable, and the energy transfer from the probe to the

Table 1
Quantitative XRD results (wt.%) for selected size fractions of ores and experimental products.

Mineral	Ore or experimental product				
Ore	Ore 1	Ore 1	Ore 1	Ore 3	Ore 3
Product ID[a]		Exp 3, Setup 1, 18 min	Exp 3, Setup 1, 18 min		Exp 9, Setup 1, 6 min
Size range	−150 + 75 μm	−150 + 75 μm	CS6	−150 + 75 μm	CS6
Hematite	62	75	48	63	39
Goethite	31	24	47	30	48
Kaolinite	3	–	4	4	10
Gibbsite	–	–	<1	2	2
Quartz	4	<1	<1	<1	<1
Halite	–	–	<1	–	–

[a] The product ID consists (in sequence) of the experiment number, the setup number and the duration of sonication.

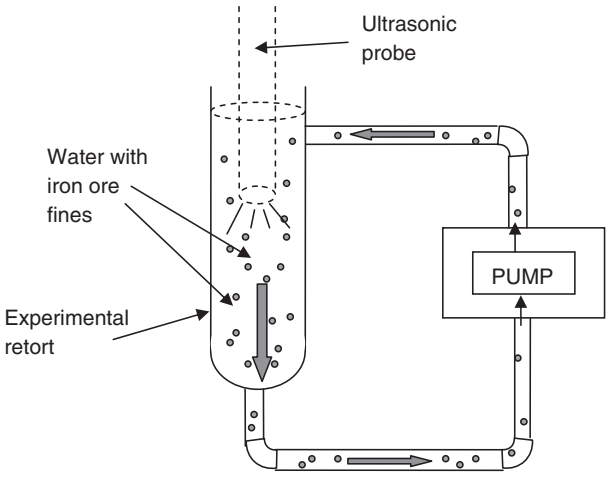

Fig. 1. Setup 1 for studying the effect of ultrasound on iron ore fines.

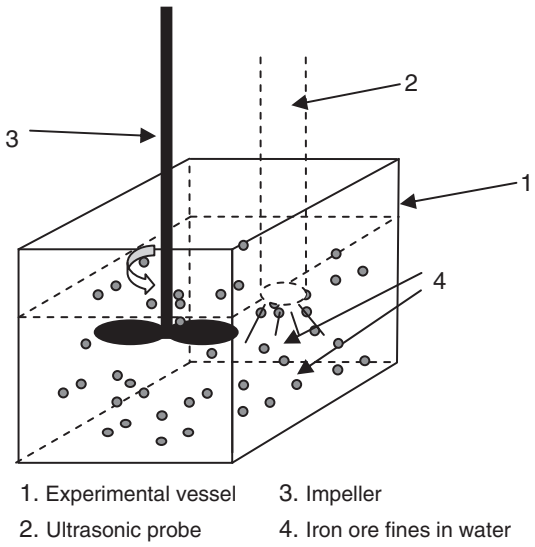

Fig. 2. Setup 2 for studying the effect of ultrasound on iron ore fines.

pulp decreased with the change from laminar to turbulent pulp movement. The impeller rotation speed was varied from 450 rpm to 830 rpm and it was observed that with increases in rotation speed the power transferred from the ultrasonic probe decreased. For example, in Exp 13 (450 rpm) the ultrasonic power was ~114 W, while in Exp 16 (830 rpm) it dropped to ~105 W. The amount of water in the vessel was about 700 ml and the amount of iron ore was approximately 140 g, so that the density of the pulp (~17% solids) was similar to that in the majority of the experiments conducted with Setup 1. Water temperature for this setup was not measured. Details of the experimental conditions for the tests are given in Table 2.

2.4. Setup 3 — static pulp

In the third experimental setup (Setup 3), the effect of high power ultrasound was studied. About 200 g of iron ore and 800 ml of water (20% solids) were introduced into the experimental retort together with an ultrasonic horn providing initially more than 1700 W of power. The experimental setup is shown in Fig. 3 and the test conditions are given in Table 2. It was observed that the pulp temperature increased from room temperature significantly during the Setup 3 experiments (to 60 °C for Exp 20 and 73 °C for Exp 22), while the power supplied to the pulp decreased. For example, at the beginning of Exp 22, the power was 1750 W, but by the end of the test it had decreased to 1500 W. While there was no pumping or stirring of the pulp during these experiments, it was observed that fine particles were moving together (entrained) with water currents created by the strong ultrasonic field, while the larger particles were not moving and settled out on the bottom of the tank.

During the cooling down period (10–15 min after the experiment) in Exp 22 on Ore 3, three distinct phases could be seen clearly in the tank: clean water on top, a jelly-like layer below the clean water, and settled solids on the bottom. Ore 3 had gibbsite present and it is suspected that the jelly-like fraction may have been coagulated fine gibbsite.

Table 2
Experimental conditions for performed tests.

Exp. No.	Ore	Product ID[a]	Rotation speed (rpm)
Setup 1			
1	Ore 1	Exp 1, Setup 1, 2 min	NA
2	Ore 1	Exp 2, Setup 1, 6 min	NA
3	Ore 1	Exp 3, Setup 1, 18 min	NA
4	Ore 1	Exp 4, Setup 1, 2 min, 41% solids	NA
6	Ore 2	Exp 6, Setup 1, 2 min	NA
7	Ore 2	Exp 7, Setup 1, 6 min	NA
8	Ore 3	Exp 8, Setup 1, 2 min	NA
9	Ore 3	Exp 9, Setup 1, 6 min	NA
Setup 2			
13	Ore 1	Exp 13, Setup 2, 40 s	450
14	Ore 1	Exp 14, Setup 2, 5 min	610
15	Ore 3	Exp 15, Setup 2, 5 min	610
16	Ore 4	Exp 16, Setup 2, 5 min	830
19	Ore 1	Exp 19, Setup 2, 5 min, R[b]	610
21	Ore 1	Exp 21, Setup 2, 5 min, 46% solids	820
Setup 3			
20	Ore 1	Exp 20, Setup 3, 3.5 min	NA
22	Ore 3	Exp 22, Setup 3, 5 min	NA

NA — not applicable.
[a] The product ID consists (in sequence) of the experiment number, the setup number, and the duration of sonication. For experiments 4 and 21, the pulp density (41% and 46% solids respectively) was higher than the pulp density used for the other tests (17% solids).
[b] Rotation only — no ultrasonics in this test.

2.5. Analysis

Products from each experiment were sized using standard laboratory wet and dry screening methods, including sub-sieve sizing (less than 38 μm) using the modified CSIRO cyclosizing technique

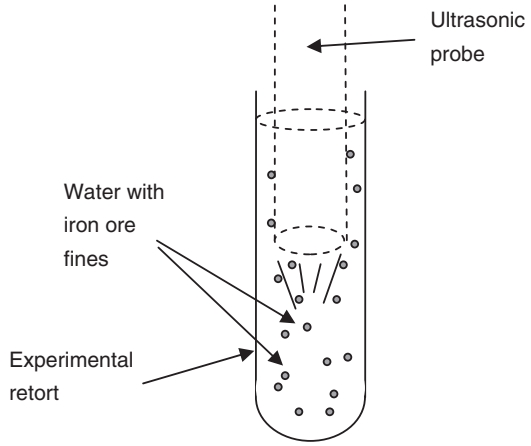

Fig. 3. Setup 3 for studying the effect of ultrasound on iron ore fines using a high power ultrasonic probe.

developed by Kelsall et al. (1974). Size fractions CS1–CS5 were obtained by cyclosizing −38 μm feed on five consecutive small hydrocyclones with consecutively reducing cut size. Two further size fractions (CS6 and CS7) below those obtained by conventional cyclosizing (CS1 to CS5) were collected using a continuous centrifuging of the last small hydrocyclone overflow (CS6) and a multiple decantation procedure (CS7). The average calculated plot sizes for different size fractions of Ore 1 are shown in Table 3.

Sub-samples of the feeds and products (including all size fractions) were assayed for a suite of elements using a standard iron ore XRF method — elements of interest included iron, silicon, and aluminium.

Quantitative mineral phase data was also obtained using quantitative XRD analysis (the Rietveld method).

3. Results and discussions

3.1. Setup 1 — Ore 1 and Ore 2

Size distributions of products from Exps 1–4 with Ore 1 using Setup 1 are shown in Fig. 4. It is clear that with increasing duration of sonication the amount of material in the larger size fractions (>106 μm) decreases, while the amount of fines (CS6 and CS7) increases. The difference in exposure time between Exps 1 and 2 is a factor of three. However, the difference in the increase of the combined CS6 + CS7 fraction is only 32%. It seems that the effectiveness of fine removal with ultrasonic treatment significantly decreases with time and we speculate that for each ore type and size fraction there is an optimum exposure time needed to achieve optimum de-agglomeration.

In Exp 4, the duration of the ultrasound treatment was the same as in Exp 1, but the amount of ore added to the pulp was three times greater. The de-agglomeration effect was slightly reduced in Exp 4 compared with Exp 1 — there was more material in the larger size fractions and less in the combined CS6 + CS7 fraction.

In Fig. 5, the iron, silica and alumina contents of the original ore and of the products from Exps 1, 2 and 3 are presented. It is interesting to see that the iron grade for most size fractions in all three tests has increased. This effect has been described previously (Donskoi et al., 2007b). While somewhat counter-intuitive, the increase of iron grade in the majority of size fractions is possible if combined with an appropriate change in the size distribution. The effect is explained by the shift in the size distribution because of liberation/de-agglomeration of fine components (which are lower in iron grade than the coarse fractions, but higher in iron grade than the fine fractions) from the coarser fractions. This shift has the effect of increasing the iron grade of the coarser fractions (due to the loss of the lower grade fines) and at the same time upgrading the finer fractions (due to the redistributed higher grade material from the coarser size fractions).

To understand this effect we provide a simplified example in Fig. 6 (Donskoi et al., 2007b). In the example, there are only two size fractions. The first size fraction, which is coarse, consists of two components, one with 60% iron grade and the other, assumed more fragile, with 40% iron grade. The fine size fraction consists of 20% iron grade fines. Let us imagine that during an experiment, the 40% iron grade component of the sample has been reduced in size, and therefore has been transferred from a coarse to a fine size fraction. Before the experiment, the iron grade of the coarse fraction was 50% (average of 60% and 40%) and the iron grade of the fine size fraction was 20%.

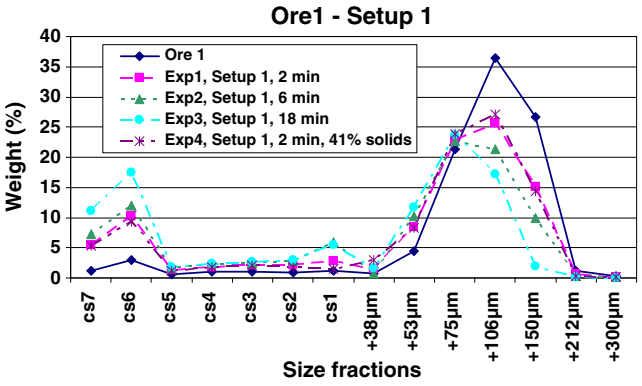

Fig. 4. Weight distributions by size for Ore 1 and the products of experiments 1–4 (Setup 1).

After the experiment, the iron grade of the coarse size fraction became 60% and the iron grade of the fine size fraction became 30%. Therefore, in this example, there was a simultaneous increase of iron grades in the coarse and fine size fractions. Again, the effect may occur only when the component of the ore which moves from the coarser to the finer size fraction has an average iron grade lower than that of the coarse size fraction, but higher than that of the fine size fraction.

It can be seen from Fig. 5a that the longer the ultrasonics is applied, the higher is the iron grade of the CS6 and CS7 size fractions, which means that the longer the sonication, the higher the iron grade of the ultrafine particles being removed from the larger size fractions.

To make decisions about the appropriate cut size to be used during de-sliming after sonication, it is important to understand clearly what the iron, silica and alumina grades of the product (the hydrocyclone underflow) will be, as well as the iron recovery to the underflow or loss to the overflow after de-sliming. In Fig. 7, the cumulative calculated iron, silica and alumina grades are shown for the progressive removal of size fractions from finest to coarsest (left to right) from Ore 1, simulating de-sliming with cuts at progressively coarser cut sizes. Without de-sliming (point "CS7" in Fig. 7), the corresponding data point for all graphs for each particular component should coincide (equivalent to the untreated feed, Ore 1). As can be seen these points for alumina and silica are very close, while for iron there is a spread of 0.36% Fe. This could be caused by slight differences in samples or small errors in iron assays within different size fractions. The fact that for alumina and silica these points are very close supports the hypothesis of errors in iron assays within different size fractions (if the samples were different alumina and silica would be also different). To reduce the effect of the error, some graphs for iron are given as both original and adjusted based on the difference in CS7 points (see Fig. 7b).

It can be seen from Fig. 7 that the most significant increase in iron grade and decrease in alumina and silica content of product occurs if the CS6 and CS7 size fractions are removed following a 2 min ultrasonic treatment (actual time of exposure is 20 s). Furthermore, the rate of these changes is significantly reduced with longer ultrasonic treatment. For the +150 μm size fraction, a significant reduction of the de-slimed product iron grade and a significant increase in silica content in the product of Exp 3 (18 min ultrasonic exposure) can be seen. The amount of material in the +150 μm size fraction (see

Table 3
Average calculated sizes for different size fractions of Ore 1.

Size fraction	+106 μm	+75 μm	+53 μm	+38 μm	CS1	CS2	CS3	CS4	CS5	CS6
Plot size (μm)	178.3	89.2	63.1	44.9	34.3	27.3	20.2	13.7	10.2	4.9

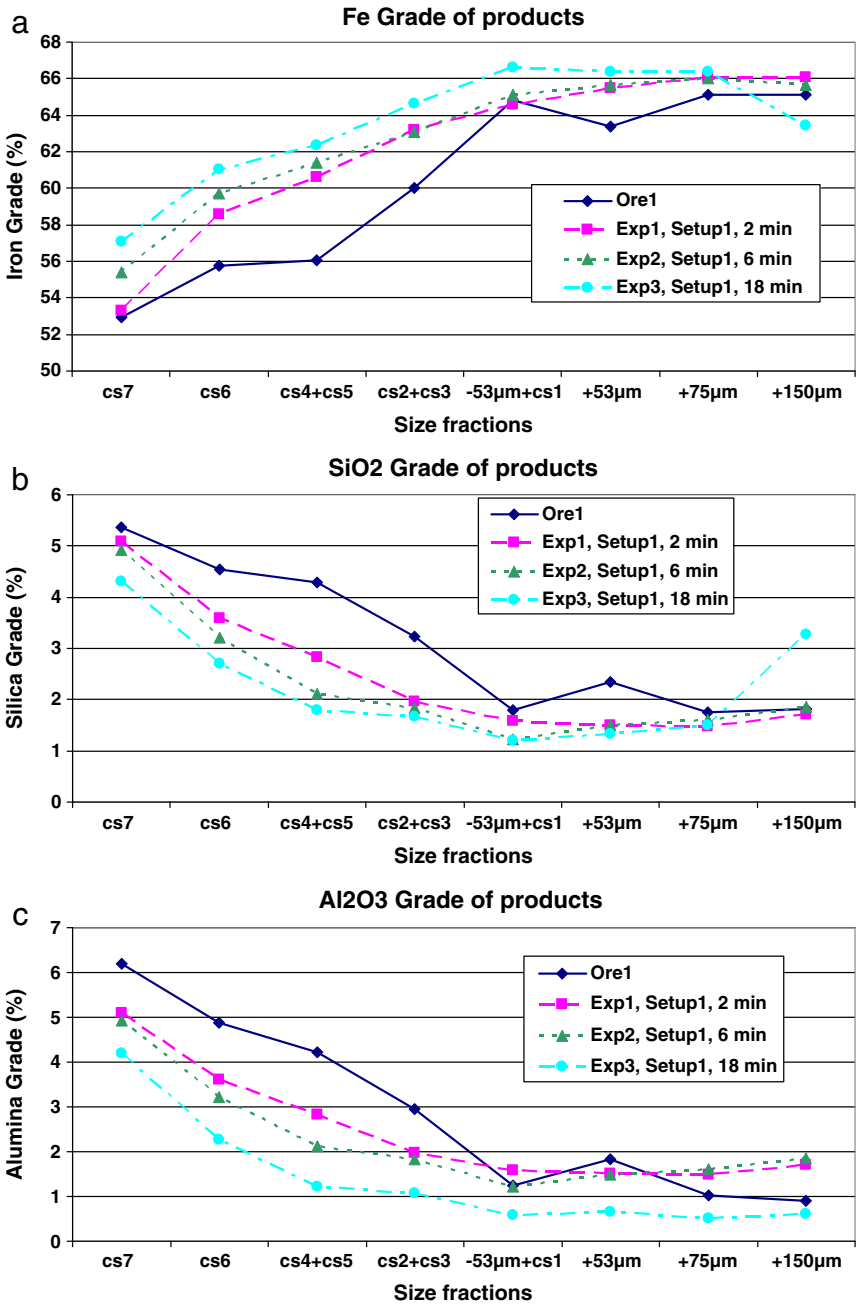

Fig. 5. Grades of Fe (a), SiO_2 (b) and Al_2O_3 (c) as a function of particle size in Ore 1 and the products of experiments 1–3 (Setup 1).

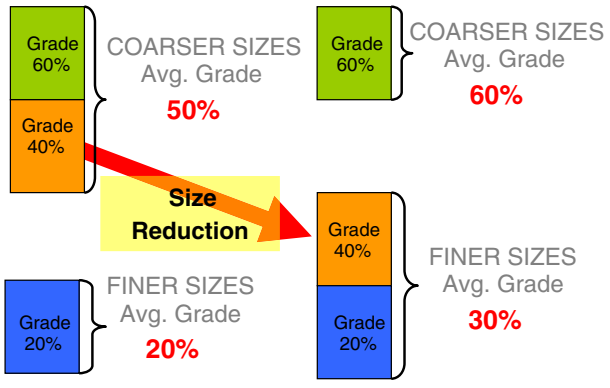

Fig. 6. Example of how the iron grade within size classes can be increased by the preferential de-agglomeration of medium-grade fines (reproduced from Donskoi et al., 2007a).

Fig. 4) in Exp 3 was significantly less than in the +150 µm size fractions from other tests. The reduction in iron and increase in silica content in this size fraction suggests that some hard silicates (probably quartz) may be less affected by ultrasonics than the other major iron-bearing minerals.

The iron grade of the de-slimed product for the 2 min treatment (Exp 1) was not very different from the iron grade of the de-slimed product after a 6 min treatment (Exp 2). However, the iron grade corresponding to Exp 3 (18 min treatment) was significantly different from the iron grades corresponding to Exps 1 and 2. As can be seen in Table 4, the iron grade of the de-slimed product for Exp 3 (if the CS6 and CS7 size fractions are removed) is 1.18% higher than that for similarly de-slimed Ore 1 without ultrasonic treatment (65.96% against 64.78%, the head iron grade being 64.38% Fe). Silica would decrease from 1.87% to 1.53% SiO_2 (18% reduction, 1.99% SiO_2 in the head) and alumina would decrease from 1.12% to 0.63% Al_2O_3 (44%

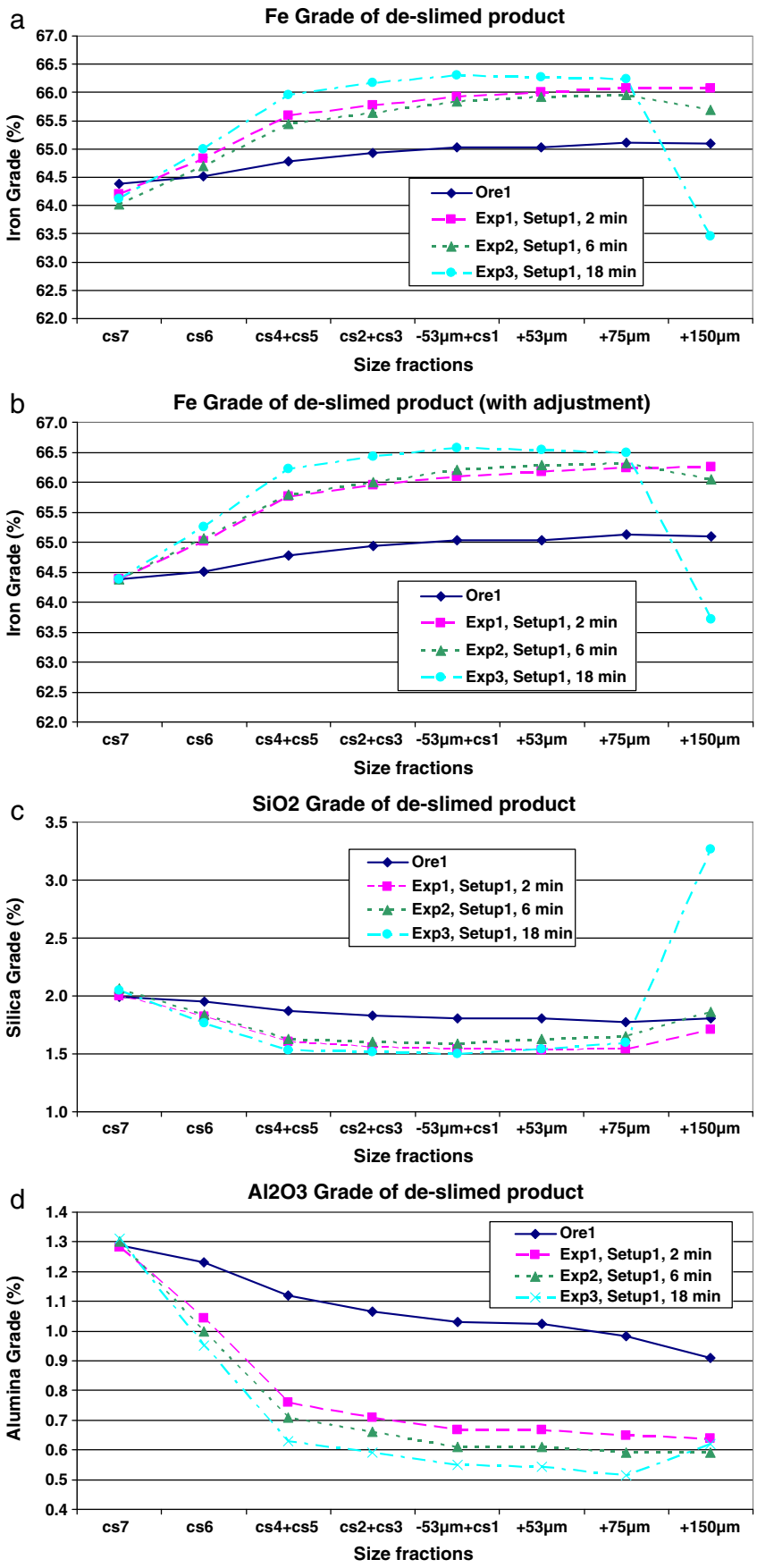

Fig. 7. Calculated grades of Fe (a), Fe with adjustments (b), SiO_2 (c) and Al_2O_3 (d) for Ore 1 and the products of experiments 1–3 (Setup 1) after the progressive removal of size fractions from left-to-right (simulated ideal cut de-sliming, size fractions below those indicated on the graph are removed, i.e., CS7: no removal, CS6: CS7 removed, CS4 + CS5: CS7 and CS6 removed, etc.).

Table 4
Product grades and recoveries of iron, silica and alumina after calculated de-sliming using Ore 1.

Sample	Size fractions removed	Grade of de-slimed product (%)			Recovery (%)		
		Fe	SiO_2	Al_2O_3	Fe	SiO_2	Al_2O_3
Ore 1	None	64.38	1.99	1.29	100	100	100.0
	<CS6	64.52	1.95	1.23	99.1	96.9	94.5
	<CS5	64.78	1.87	1.12	96.5	90.2	83.3
	<CS3	64.93	1.83	1.07	95.1	86.7	78.0
Exp 1, Setup 1, 2 min	<CS6	64.83	1.82	1.04	95.5	86.2	77.1
	<CS5	65.59	1.61	0.76	86.2	67.9	50.1
	<CS3	65.78	1.56	0.71	83.3	63.5	45.0
Exp 2, Setup 1, 6 min	<CS6	64.71	1.83	1.00	93.7	82.5	71.2
	<CS5	65.44	1.63	0.71	82.5	63.9	43.9
	<CS3	65.65	1.61	0.66	78.7	59.9	39.0
Exp 3, Setup 1, 18 min	<CS6	64.99	1.76	0.95	90.2	76.7	64.7
	<CS5	65.96	1.53	0.63	73.5	53.5	34.3
	<CS3	66.17	1.52	0.59	69.5	50.0	30.5

reduction, 1.29% in the head). The reduction of alumina is significant. The total reduction of alumina relative to the initial ore is 51%, so if the alumina grade is critical, ultrasonic treatment can provide a significant improvement for ores with similar mineral composition.

However, the trade off for iron grade improvement is a reduction in iron unit recovery to the de-slimed product (see Table 4). Table 4 and Fig. 8 show the cumulative calculated iron, silica and alumina recoveries for the progressive removal of size fractions from finest to coarsest (left to right) from Ore 1 and the products of the experiments 1–3, simulating de-sliming with cuts at progressively coarser cut sizes (removal is assumed for the size fractions lower than is indicated on the graph, that is, CS7: no removal, CS6: CS7 removed, CS4–CS5: CS7 and CS6 removed and so on).

It can be seen from Fig. 8 and Table 4 that if (calculated) de-sliming is applied to the product of Exp 3, by removing the CS6 and CS7 size fractions, the relative amount of alumina remaining will be just 34.3% of that in the head. This is 49% less than if the same de-sliming was applied to Ore 1 without ultrasonic treatment (83.3% Al_2O_3 recovery). However, the iron recovery would be 73.5%, which is 23% less than for Ore 1 without ultrasound application (96.5% iron recovery). For Exp 1 (under the same conditions) the iron recovery would be 86.2%, while the recovery of alumina would be 50.1%, which is 33% less than that for Ore 1 without ultrasound application.

In Fig. 9, the data from Figs. 7 and 8 are combined into calculated grade-recovery plots of iron, silica and alumina product grades against iron recovery for perfect cut de-sliming. It can be seen that after de-sliming, the iron grades of ultrasonically treated samples (see Fig. 9a for corrected comparison) are generally higher than those of untreated samples at the same recovery. To avoid the interference of differences in initial iron grades of the samples, Fig. 9a shows the case where all the experimental iron grade data has been shifted to match the initial iron grade of the head sample.

The data in Table 4 and Fig. 9 show that to obtain the same iron recovery as that after calculated de-sliming of Ore 1 without ultrasonic treatment, the separation/de-sliming after ultrasonic treatment has to be performed at a finer cut size. For example, the iron recovery of 86.2% in Exp 1 corresponds to removal of the CS6 and CS7 size fractions, and the corresponding iron grade will be 65.59% (65.76% if normalised). In the untreated original ore, a similar iron recovery of 87.1% corresponds to de-sliming at 53 μm, giving an iron grade of 65.12% Fe. It is noted that with approximately the same iron recovery, the product iron grade of Exp 1 with ultrasonic treatment is higher by 0.5% (for lower recoveries this difference would be much higher) and the alumina content is significantly lower, i.e. 0.76% Al_2O_3 compared with 0.98% Al_2O_3. For an iron recovery somewhere around 70%, the difference in product iron grade between treated and untreated ores would be more than 1% Fe, while the alumina content of the treated ore would drop to approximately 0.6% Al_2O_3. With even finer de-sliming of the treated ore (finer than the de-sliming of the untreated ore, i.e. further right on the graph in Fig. 9), both iron grade and recovery can be improved simultaneously. In Fig. 9a, circles "A" and "B" correspond to the situation where the iron grade and recovery are improved at the same time, where desliming applied to ultrasonically treated ore is finer than desliming applied to untreated ore.

It is important to note that for higher (>70%) iron recoveries (finer cut sizes), shorter ultrasonic treatment is more efficient from an iron grade/recovery point of view (see Fig. 9a). However, for lower (<70%) iron recoveries (coarser cut sizes) with longer durations of treatment, the product iron grade can be significantly higher (>66.3% Fe) and the alumina grade significantly lower (Fig. 9c). Furthermore, after ultrasonic treatment, the percentage of alumina removed is much higher than the percentage of silica removed, so the alumina/silica ratio in the products after ultrasonic treatment will be much lower than without ultrasonic treatment (See Fig. 10a). This could be advantageous for iron producers in the subsequent agglomeration and metal production processing steps.

The relative behaviour of alumina recovery versus iron recovery for Ore 1 is given in Fig. 10b. For an iron recovery of ~80%, ultrasonic treatment reduces the alumina recovery from ~60% to less than 40%.

In general, similar results were obtained for the other hematitic/goethitic ores tested, but some differences were noted. The main results for ultrasonic treatment of Ore 2 using Setup 1 are given in Figs. 11–13. By comparing Figs. 5a and 12, it can be seen that the change in iron grade within each size fraction after sonication is different between Ore 2 and Ore 1. For Ore 1 the increase in iron grade after sonication for fine size fractions (<CS2) was significant (4–6%) and the increase for coarse size fractions was much lower (<2.5%). For Ore 2 the change in the iron grade for fine size fractions (<CS2) was lower (<1.0%) than for coarse (+53 μm) size fractions (up to 2%). Following simulated desliming, it is apparent from Figs. 13 and 9a that sonication has led to a greater improvement in the iron grade of Ore 2 relative to Ore 1 (up to 2.5% and 1.5%, respectively) at iron recoveries of up to 50%. However, at high iron recoveries (70–90%), the improvement is lower for Ore 2 than for Ore 1. This is attributed to differences in the size distributions of Ore 1 and Ore 2 coupled with the different magnitudes of iron grade improvements within coarser and finer size fractions achieved by sonication. Points A and B in Fig. 13 also demonstrate the possibility for simultaneous increase of iron grade and recovery using sonication.

3.2. Setup 2 — Ore 1

Using Setup 2, Exps 13, 14, 19 and 21 were performed with Ore 1 (see Table 2 for details of the experimental conditions). The results are presented in Fig. 14.

At this stage it is necessary to introduce and make clear three distinct terms that will be used further in the discussion. The first one is "specific effectiveness of fines removal" which will mean the amount of production of CS6 + CS7 size material per weight unit of iron ore, so it is represented by the percentage of CS6 + CS7 size material created during treatment. The second term is "total effectiveness of fines removal" which will mean the overall amount of production of CS6 + CS7 size material in the reactor. Finally, "energy efficiency" which will mean the amount of energy spent to remove certain amount of CS6 + CS7 size material from a weight unit of iron ore.

Fig. 14 shows that the specific effectiveness of fines removal under Setup 2 was surprisingly low in comparison with Setup 1. The data show that 5 min exposure under Setup 2 (Exp 14) was less effective (in terms of production of CS6 + CS7 size material per weight unit of iron ore) than 2 min (actual exposure 20 s) using Setup 1 (Exp 1) with pulp circulation through the system.

There are a number of possible explanations for the lower specific effectiveness of fines removal in Setup 2. Firstly, in Setup 1 the

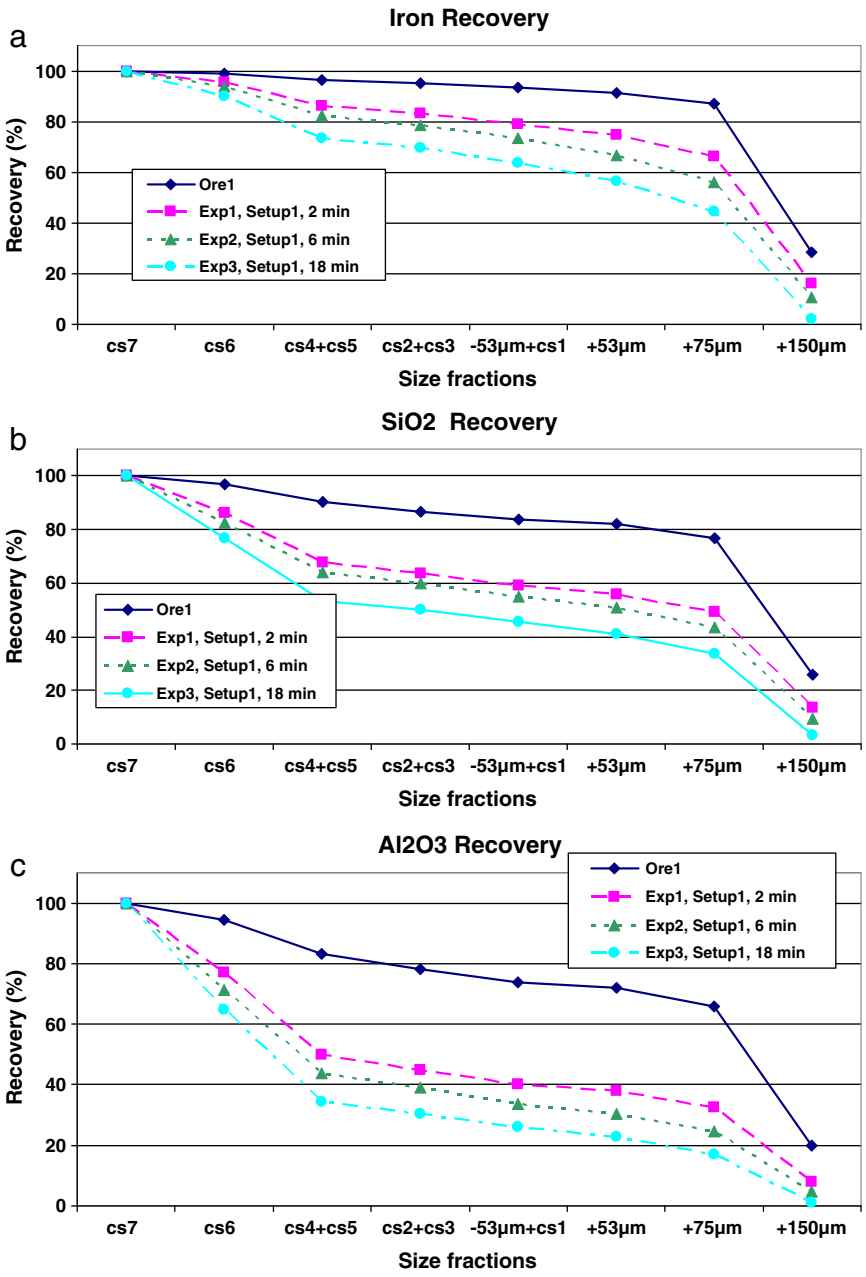

Fig. 8. Calculated recoveries of Fe (a), SiO_2 (b) and Al_2O_3 (c) for Ore 1 and the products of experiments 1–3 (Setup 1) after the progressive removal of size fractions from left-to-right (simulated ideal cut de-sliming, size fractions below those indicated on the graph are removed, i.e., CS7: no removal, CS6: CS7 removed, CS4 + CS5: CS7 and CS6 removed, etc.).

delivered power of ultrasound was greater (~150 W vs ~110 W), while the amount of ore and water was much smaller, and so was the size of the reactor. In Exp 14 (Setup 2, 5 min) there was 140.78 g of ore and 700 ml of water, whereas in Exp 1 (Setup 1) there was 24.75 g of ore and 120 ml of water. The second possible reason is that in Setup 2, the stirrer rotation was probably not sufficient for adequate mixing, so the ore partially settled on the bottom of the vessel. As it will be shown later, the effect of ultrasound on settled ore is very small. The third possible reason is that depending on the shape of the ultrasonic probe, the ultrasonic power applied to the pulp is directional, so only a limited space under and close to the ultrasonic probe is sufficiently exposed to ultrasound in Setup 2. This leads to the conclusion that it is preferable to distribute power over the treated volume evenly so that the entire pulp is equally sonicated.

It is noted that the total effectiveness of fines removal was much higher in Setup 2. The total amount of CS6 + CS7 size material produced during 6 min in Setup 1 (Exp 2) was 3.76 g while for 5 min in Setup 2 (Exp 14) it was 7.56 g, even though the delivered power of ultrasound was greater in Setup 1. There are two possible reasons for total effectiveness of fines removal being higher in Setup 2 than in Setup 1.

The first reason is quite obvious — the amount of ore in the Setup 2 (Exp 14) was much higher than in Setup 1 (Exp 2). In Exp 1 (Setup 1, 2 min, 17% solids) the amount of CS6 + CS7 size material generated was 2.85 g (11.5%). With the same time of ultrasonic treatment in the same reactor in Exp 4 (Setup 1, 2 min, 41% solids) there was 6.37 g (10.5%) generated, which is significantly more than in Exp 1. It is likely that increasing the size of reactor and increasing the amount of ore would increase the amount of CS6 + CS7 size material

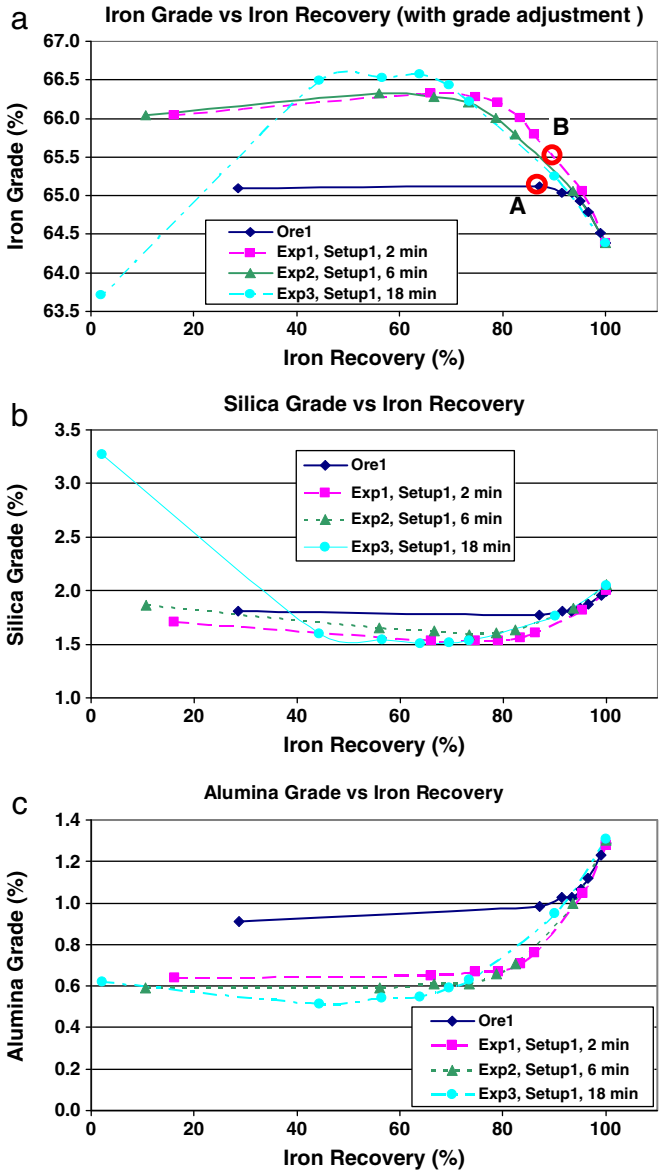

Fig. 9. Calculated grades of Fe with adjustment (a), SiO_2 (b) and Al_2O_3 (c) plotted against the calculated iron recovery for Ore 1 and the products of experiments 1–3 (Setup 1) after simulated ideal cut de-sliming.

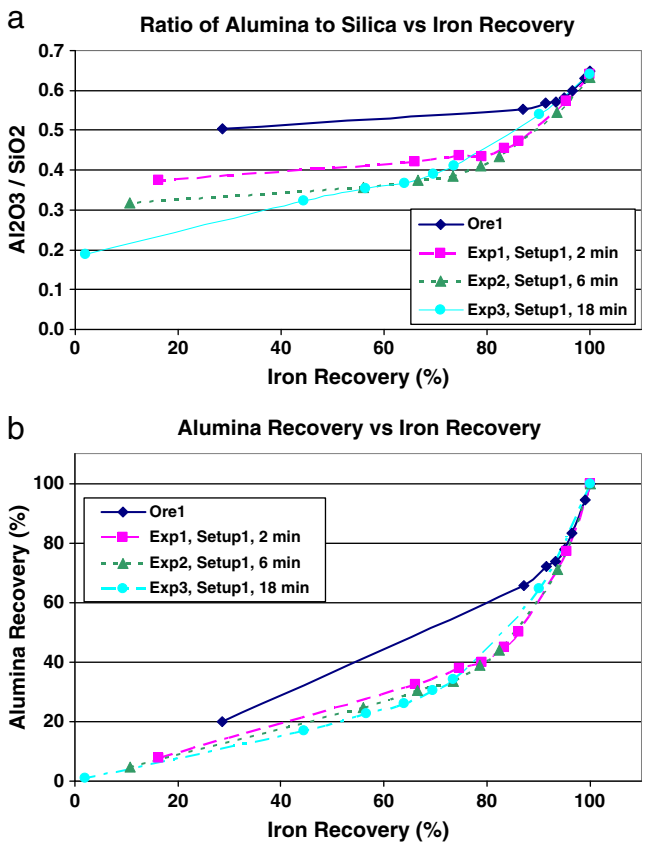

Fig. 10. a) Calculated ratio of Al_2O_3 to SiO_2 and b) calculated recovery of Al_2O_3 — plotted against the calculated iron recovery for Ore 1 and the products of experiments 1–3 (Setup 1) after simulated ideal cut de-sliming.

generated to a certain extent. However, optimisation of reactor size and pulp densities for certain types of reactors (from total effectiveness of fines removal point of view) will be required and this should be a topic for a separate study.

The second possible reason for the fact that total effectiveness of fines removal is higher in Setup 2 than in Setup 1 is that in Setup 2 the rotation creates a highly turbulent flow which helps to efficiently remove disintegrated material from the particle surface. To better understand this effect it is convenient to subdivide the effect of ultrasound on a particle into two phases, the first one being the selective disintegration of the particle due to cavitation, and the second phase being the removal of the disintegrated material from the surface of the particle. If this physical model is taken into consideration, it is clear that in Setup 1, with almost laminar flow removal of the disintegrated material from the surface of the particle is much less efficient than in Setup 2. It should also be remembered that high pressure and temperature during cavitation may not only disintegrate soft material, but fuse it as well (Pandey et al., 2010). This fusion has the opposite effect to what is desired during ultrasonic treatment, so the efficient removal of disintegrated material from particle surface to avoid fusion is advantageous. Also, it should not be forgotten that such rotation significantly increases particle abrasion and attrition.

In Exp 19, rotation only without ultrasound was applied for 5 min. There was almost no difference in product size distributions between Exps 19 and 13 (ultrasound plus rotation for 40 s, see Fig 14). The percentage of CS6 + CS7 material in Exp 13 was 6.41%, while in Exp 19 it was 6.24% (for 7.5 times longer duration). This demonstrates that ultrasound significantly improves de-agglomeration efficiency during rotation, while utilisation of rotation alone is not as efficient. This conclusion is also supported by previous work conducted with Ore 2 in an ultrasonic bath (Donskoi et al., 2010b). In the original

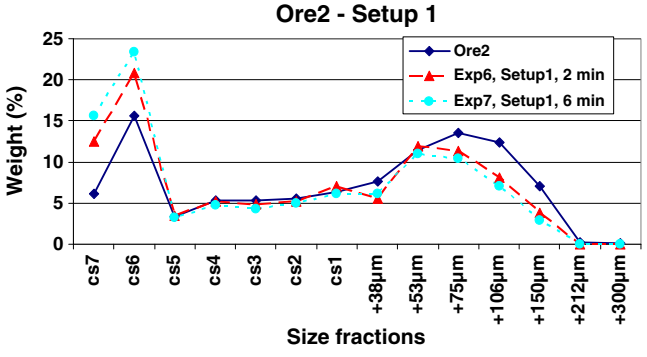

Fig. 11. Effect of sonication time on particle size distribution of Ore 2 (Setup 1).

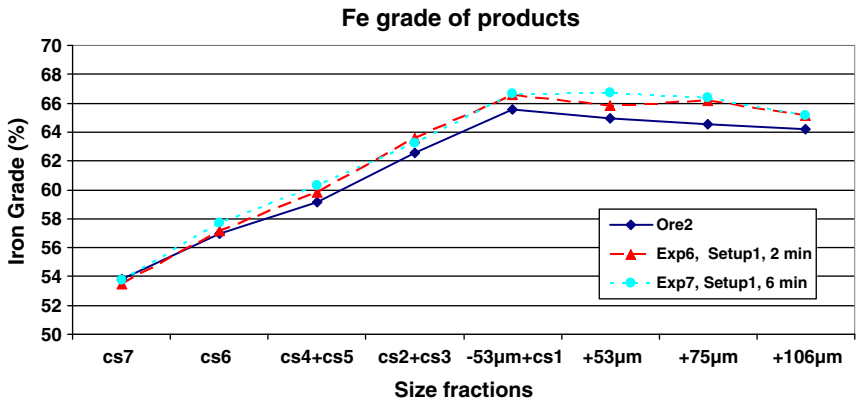

Fig. 12. Fe grade as a function of particle size for Ore 2 and test products from experiments 6 and 7 (Setup 1).

Ore 2, the percentage of CS6 + CS7 fractions was 21.7%. With the utilisation of ultrasound and rotation, the weight in these fractions increased by 6.64%. However, when only rotation was used and other conditions remained the same, the weight in these fractions only increased by 2.47%. Remarkably, when only ultrasound was used (without rotation), the increase was much lower (0.9%). Without stirring, the iron ore created a dense (still washable but harder than usual) cake on the bottom of the vessel, with low permeability for the ultrasonic waves and a low level of cavitations. This clearly demonstrated that when ore is packed on the reactor bottom and not suspended in the water the effect of ultrasound is very low. Both sonication and suspension (preferably with intensive rotation) are needed.

Exp 21 was performed with a significantly higher pulp density in comparison with Exps 13, 14 and 19 (46% solids vs. 17% solids). Once again, the specific effectiveness of fines removal of ultrasound was less in Exp 21 than in Exp 14 (with lower pulp density) where all other parameters were the same.

3.3. Setup 3 — Ore 1

With Setup 3, more water (800 ml) and ore (206.79 g) was used compared to Setup 1, and the total power was more than 10 times higher. Power densities below the ultrasonic horn (power per unit volume) for Setup 1 and Setup 3 were quite similar, as the diameter of the ultrasonic horn in Setup 1 was 12.7 mm and its area was ~1.6 cm^2 (94 W/cm^2) while in Setup 3 the probe diameter was ~3.5 cm and its area was ~12.3 cm^2 (138 W/cm^2).

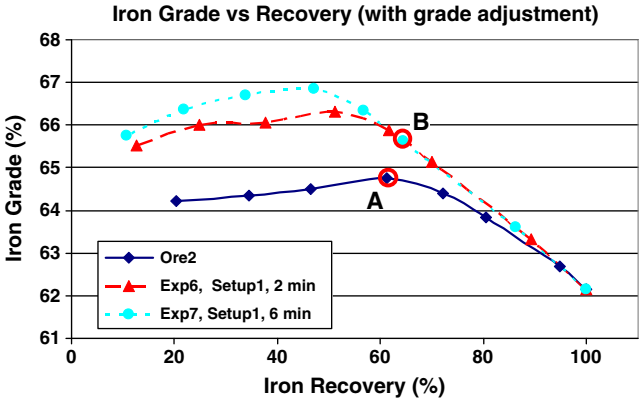

Fig. 13. Calculated iron grade (adjusted) plotted against the calculated iron recovery for Ore 2 and the products of experiments 6 and 7 (Setup 1) after simulated ideal cut de-sliming.

In Setup 3 pulp was continually affected by ultrasound while in Setup 1 pulp was affected by ultrasound for only one/sixth of the time. So if normalisation on effective time and on affected volume is performed the ultrasonic power per unit volume is higher in Setup 3 (1700/800 = 2.125 W/ml) than in Setup 1(150/20/6 = 1.25 W/ml).

Exp 20 was performed with Ore 1 under Setup 3 (3.5 min, high power ~1750–1500 W). The results given in Fig. 15 show that the size distribution of the product from Exp 20 was approximately the same as for Exp 2 (Setup 1, 6 min, but the effective exposure was 1 min). The chemical compositions of the different size fractions in the products from Exp 20 (not shown here) were similar to those of the size fractions for Exp 2. The grade and recovery figures (not shown here) were also comparable.

The specific effectiveness of fines removal of ultrasound in Exp 20 was significantly less than in Exp 3 (Setup 1, 18 min, effective exposure 3 min) and much higher than in Exp 14 (Setup 2, 5 min).

We consider now why Setup 3 proved to have lower specific effectiveness of fines removal than Setup 1. First of all it should be noted that even though power density under ultrasonic pole in Setup 3 was slightly higher (138 W/cm^2) than in Setup 1 (94 W/cm^2), the average spatial power density in Setup 1 (150/20 = 7.5 W/ml) was much higher than in Setup 3 (1700/800 = 2.125 W/ml). Furthermore, the mixing in Setup1 was much better than in Setup 3 where only slight mixing occurred due to water currents induced by the ultrasonic field. As a result, in Setup 1 the disintegrated material is removed more efficiently (and does not have time to fuse) so it is not protecting the soft parts of the particle from further disintegration. Also, in Setup 1 the entire sample is equally exposed to ultrasound, while in Setup 3 there is a high probability that the lower layers (with heavier particles) are less exposed to

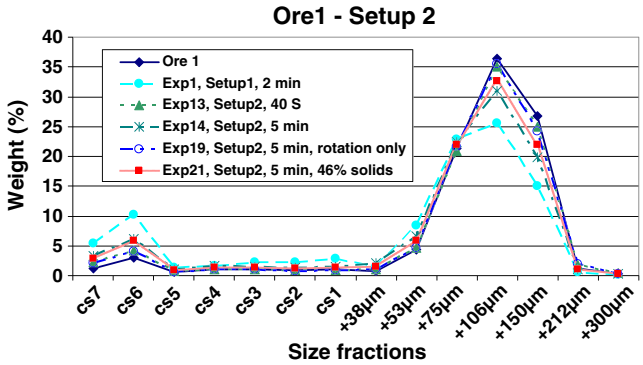

Fig. 14. Weight distributions by size for the products of experiments 13, 14, 19 and 21 (Setup 2) compared with the original Ore 1 and the product of experiment 1 (Setup 1).

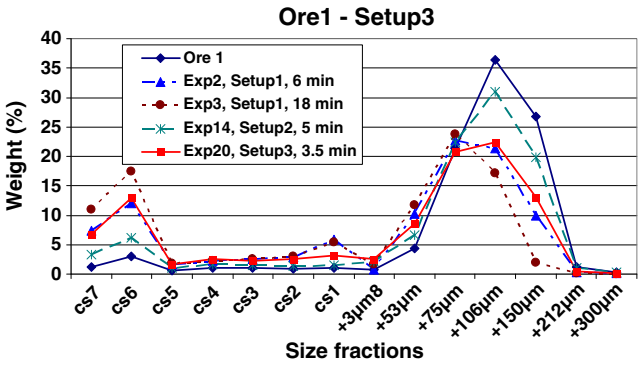

Fig. 15. Weight distributions by size for the product of experiment 20 (Setup 3) compared with the original Ore 1 and selected test products using Setups 1 and 2.

the ultrasonic field than the upper layers (with lighter particles closer to the ultrasonic pole).

There is also another possible reason for the ultrasound being more specific effective in Setup 1. In dispersed media, the ultrasonic power density decreases with increasing distance from the ultrasonic source. In Setup 1 all the slurry passes through the area near the ultrasonic probe, while in Setup 3 only a portion of the slurry is exposed to the high power density area.

It should be noted that energy efficiency (energy spent to remove a certain amount of CS6 + CS7 size material per weight unit of iron ore) is actually higher in Setup 3 in comparison with Setup 1. As discussed above the percentage of removed CS6 + CS7 size fraction in Exp 20 (Setup 3, 3.5 min) was approximately the same as in Exp 2 (Setup 1, 6 min). The energy spent per weight unit of ore in Setup 3 (1700 W∗3.5 min/206.79 g = 28.8 W min/g = 1726 J/g) was lower than in Setup 1 (150 W∗6 min/24.75 g = 36.4 W min/g = 2182 J/g). Again, increasing the amount of ore or increasing the size of reactor could increase energy efficiency to a certain extent but optimisation of the reactor was not a part of this study.

3.4. Tests with Ore 3

The behaviour of Ore 3 during ultrasonic treatment in Setup 1 was different from that of Ore 1 and Ore 2 in terms of the generation of ultrafines (see Fig. 16). The first significant difference is that the amount of ultra fines generated using Ore 3 was significantly less than that generated using Ore 2 (see Fig. 11). Using Ore 3 with Setup 1 (Exp 8), 7.2% of CS6 + CS7 material was generated after a 2 min treatment, while for Ore 2 (Exp 6, 2 min) 11.6% of CS6 + CS7 material was generated, and for Ore 1 (Exp 1, 2 min) 11.5% of CS6 + CS7 material was generated. When treated for 6 min with Setup 1, Ore 3 generated 9.2% of CS6 + CS7 material (Exp 9), while Ore 2 and Ore 1 generated 17.3% (Exp 7) and 15.2% (Exp 2) of CS6 + CS7 material respectively.

The size distributions for the experiments with Ore 3 are shown in Fig. 16. The specific effectiveness of Setup 2 (Exp 15, 5 min treatment) is lower than that for Setup 1 (Exp 8, 2 min treatment, actual exposure 20 s), while the specific effectiveness of the high power treatment using Setup 3 (Exp 22, 5 min) is higher than that for Setup 2 but lower than for Setup 1.

It is interesting to compare the differences in the size distributions for the products of Ore 3 under different setups (see Fig. 16). In Setup 1, the decrease of the mass of the −53 + 38 μm size fraction and the simultaneous increase of the mass of the CS1 fraction is quite prominent, while the size distributions for Setups 2 and 3 follow the initial size distribution with only minor differences. Chemical analysis has shown that CS1 has the highest iron grade compared to other size fractions (see Fig. 17), which generally means that it has the highest percentage of hematite. The possible explanation for the difference in size distributions is that Setup 1 results in the disintegration of more single mineral grains (liberated hematite particles), while Setups 2 and 3 result in less liberated disintegration. For Ore 1, an increase in the CS1 size fraction can also be observed for the 6 and 18 min treatments using Setup 1 (see Fig. 4). Thus, the increased liberation of CS1 particles may also be associated with periodical (cyclical) exposure to ultrasound in Setup 1.

It is noted in Fig. 17 that 2 min sonication using Setup 1 (Exp 8) did not produce any significant change in the iron grades of the −53 μm size fractions relative to the untreated Ore 3 feed, which was not the case with Ore 1 (see Fig. 5a, Exp 1) and Ore 2 (see Fig. 11, Exp 6). However, after further sonication (Fig. 17) in Setup 1 (Exp 9, 6 min) and in Setup 3 (Exp 22, 5 min), the iron grades of the individual size fractions increased relative to the initial ore. Also for Ore3 (and likewise for Ore1 and Ore2), after simulated desliming by removing the CS6 and CS7 fractions, the loss of iron units (~7.9%, Exp 9) is much lower than the loss of silica (~19.2%, Exp 9) and alumina (~22.8%, Exp 9).

3.5. Tests with Ore 4

The effect of ultrasound on particles significantly larger than those previously considered was studied using Ore 4. Setup 1 was not suitable for such large particles, so Ore 4 (−2000 + 1000 μm) was processed using Setup 2. To see clearly the effect of ultrasound a graph of the differences between the distributions for the product of Exp 16 and the original Ore 4 is provided (Fig. 18; size distributions for the product of Exp 16 and the original ore both have a very significant +300 μm component and comparatively much smaller

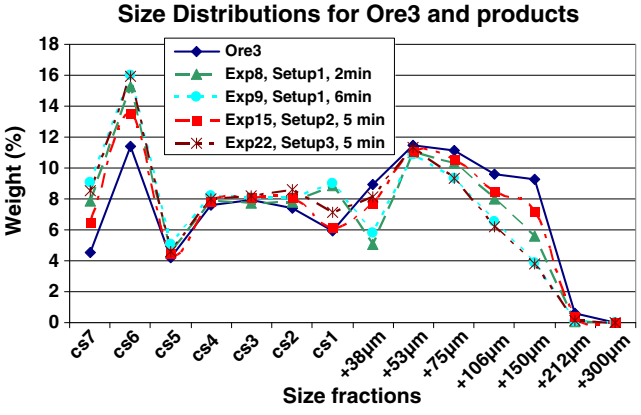

Fig. 16. Comparison of product size distributions for tests using Setups 1, 2 and 3 with Ore 3.

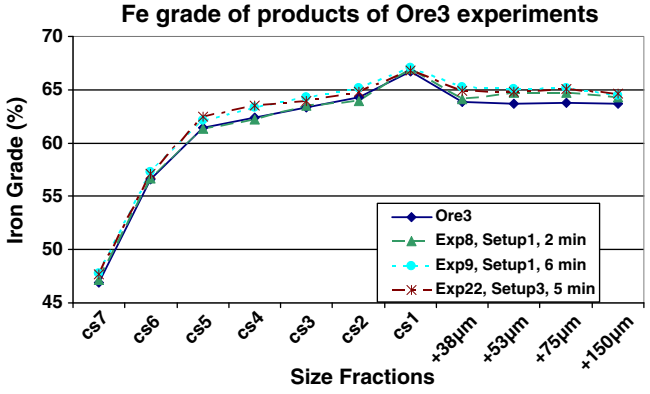

Fig. 17. Fe grade as a function of particle size for Ore 3 and selected test products using the same ore.

differences between other components which are not easy to see in overall size distributions). The effect of ultrasonics in this experiment (the amount of ultrafines produced) is significantly less than in Exp 15 with Ore 3 (see Figs. 16 and 18). There are two main reasons for this. The first is that, although stirring was continuous with Setup 2, large particles (e.g. −2000 + 1000 μm) partially settled and, as shown previously, this causes a significant reduction in the ultrasonic effect. The second reason is the particle size itself. The larger the size of the particles, the lower is their surface area for the same weight, so the effect of ultrasound is also expected to be lower.

In spite of the small observed effect (from the point of view of CS6 and CS7 fraction generation), the overall results of this experiment are quite promising. In Table 5, the results of chemical analysis for the original Ore 4 and its CS6 + CS7 and +300 μm size fractions as well as for the products of Exp 16 are given. In the majority of the experiments described earlier, after ultrasonic treatment the iron grade of the CS6+CS7 fractions either increased or remained approximately the same as in the original ore. In Exp 16, however, the iron grade of the CS6 + CS7 size fractions dropped significantly, while the iron grade of the +300 μm size fractions increased by more than 1.8%. The alumina and silica content dropped substantially as well.

If de-sliming was performed on the original ore by removing all size fractions finer than 300 μm (possibly by fine wet screening), the iron recovery would be 90.9% and the iron grade 62.04% Fe. If the same operation was performed on ultrasonically treated ore, the iron recovery would be 88.6% and the iron grade 63.9% Fe. The loss in iron units is not very significant, while the increase in the iron grade (1.76%) makes the product more attractive for iron makers.

The test results using Ore 4 are interpreted in the following manner. Due to the small surface area of Ore 4 compared to the other ores, the weight loss after ultrasonic treatment of the coarse size fractions is not large. However, all this loss can be attributed to the softest part of the ore, which has the lowest iron grade. This demonstrates that ultrasonic treatment can still be effective on relatively large iron ore particles.

Intuitively, due to the small sizes of the cavitations, the dominating surface effect of the ultrasonic treatment, and the large amount of CS6 + CS7 material produced, one may consider that the dominating particle disintegration mechanism is through the peeling off of ultra fines from larger particles.

In Exp 16, 0.78% of particles with size −150 + 53 μm were produced. To produce this quantity of particles in this size fraction only by peeling ultrafines off the +300 μm particles, at least 5.46% (7∗0.78%) of ultrafines should be produced (7/8 should be peeled out from the 300 μm particle to produce a 150 μm particle). Altogether, in the CS1 to CS7 size fractions, only 3.35% were produced. To do this rough estimation, we have taken the biggest size −150 μm in produced particle range and the smallest size −300 μm (while it is larger than 1000 μm) in disintegrated particles. With estimations that are more precise, if only peeling of ultrafines during ultrasonic treatment occurs,

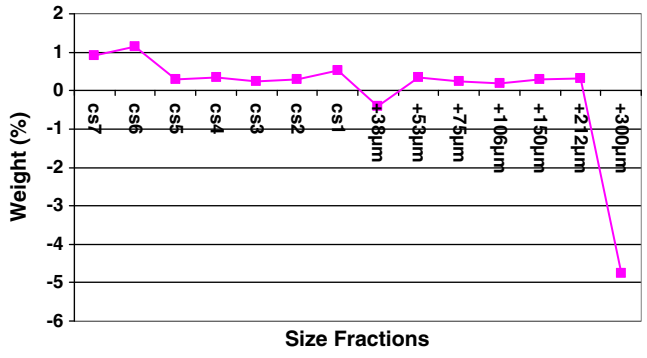

Fig. 18. Net difference between the size distribution of the product of experiment 16 (Ore4, Setup 2, 5 min) and Ore 4 without ultrasound treatment.

Table 5
Chemical analysis for the bulk Ore 4, as well as a comparison of the CS6 + CS7 and +300 μm size fractions of Ore 4 (without ultrasonic treatment) and the product of experiment 16 (Setup 2).

Sample	Fe	SiO_2	Al_2O_3
Ore 4	61.65	3.87	2.46
Ore 4 +300 μm	62.04	3.44	1.96
Exp 16, Setup 2, 5 min +300 μm	63.90	2.53	1.47
Ore 4 CS6 + CS7	55.33	5.64	5.27
Exp 16, Setup 2, 5 min CS6 + CS7	52.66	7.50	7.03

the amount of ultrafines produced should be dramatically higher than our very rough estimation — 5.46%.

Nevertheless, even such a rough estimation shows that a significant amount of +53 μm material was produced by breaking large particles into smaller pieces, not just by peeling ultrafines off the larger particles.

4. Conclusions

To study the effect of ultrasound on iron ore fines, the pulps of four different ores were treated with ultrasound under different experimental setups. In all experiments, preferential disintegration of soft minerals (associated with higher levels of alumina and silica) and deportment of this disintegrated material to the finer size fractions occurred. As a general rule, the amount of CS6 and CS7 size fractions increased, while the percentage of size fractions above 53 μm decreased. In the majority of the experiments, the portion deported from the coarser size fractions to the ultrafines (CS6 + CS7) had iron grades lower than that in the coarse size fractions, but higher than that in the combined CS6 + CS7 fractions. As a result, the iron grades of most size fractions increased after ultrasonic treatment. However, in experiment 16 using Ore 4, the iron grade of the combined CS6 + CS7 size fractions dropped significantly, while the iron grade of the +300 μm size fractions increased by more than 1.8% after ultrasonic treatment.

By modelling subsequent desliming assuming perfect cut size removal, it has been shown that the deportment of low-grade soft material from the coarse size fractions to the ultrafine size fractions can potentially improve the product iron grade after de-sliming. Furthermore, in order to achieve the same iron recovery (with a higher iron grade) that would have been achieved by de-sliming the ore without ultrasonic treatment, separation/de-sliming should be performed at a finer cut size. For every treated ore considered, there was a possibility of simultaneously increasing the iron grade and recovery by utilising ultrasonic treatment. For the ores treated in the experiments, it was calculated that the iron grade of the de-slimed ore that was pretreated ultrasonically would be up to 2% higher than the de-slimed ore without ultrasonic treatment when maintaining similar iron recoveries. There are reasons to believe that for particular low grade ores this value may rise significantly. The ores used for the experiments had relatively low amounts of silica (2.5–3.5%) and alumina (1%–3%), and it is likely that for ores with higher contents of alumina and silica the gain in iron grade with the application of ultrasound would be much higher. It is also worth noting that for all ores, the preferential removal of alumina, rather than silica, occurred after ultrasonic treatment. Therefore, if de-sliming after ultrasonic treatment is performed at a finer separation size, the final classification product will have a higher iron grade and relatively lower amounts of alumina compared to silica, while maintaining a similar iron recovery compared with conventional desliming.

In terms of physical conditions, the experimental results showed that ultrasonic treatment without stirring is inefficient, as the ore creates a dense cake on the bottom of the vessel, and this cake has a low permeability for ultrasonic waves and low levels of cavitations. For ultrasonics to be efficient, the solids should be well suspended in the

pulp and well stirred. The suspension of ore in the pulp has been shown to be a factor significantly affecting the results of ultrasonic treatment. The effect of ultrasound on lower density pulps was demonstrated to be slightly more specific effective than on high density pulps, but this difference was not critical. The increase in pulp density can in turn significantly increase the total ultrasonic effect. A comparison of the efficiency of different setups suggests that the ultrasonic power should be applied periodically so that disintegrated material can be washed away before it becomes partially fused. It is also preferable to distribute the ultrasonic power over the affected pulp volume evenly. During ultrasonic treatment, both cracking of particles into smaller pieces and peeling off of ultrafines from the larger particles take place.

For every individual iron ore, it will most likely be necessary to optimise the different parameters of ultrasonic exposure (e.g. power, time and pulp density) in order to achieve the best outcome. Our experimental results indicate that the efficiency of ultrasonic treatment significantly decreases after a threshold reaction time. For ores with high levels of fine material and high contents of ochreous goethite and kaolinite, very short ultrasonic treatment times (less than 15–20 s) can significantly improve product iron grade and recovery if the appropriate de-sliming cut size is selected.

Acknowledgments

The authors wish to thank Anthony Farmer and Paul Gwan of CSIRO Materials Science and Engineering for their help in conducting experiments at the CSIRO laboratories in Lindfield, NSW. We would like to acknowledge Ralph Holmes and Steve Suthers of CSIRO Process Science and Engineering for reviewing this paper and their useful corrections and comments.

References

Didenko, Y.T., Suslick, K.S., 2002. The energy efficiency of formation of photons, radicals and ions during single-bubble cavitation. Nature 418, 394–397.

Donskoi, E., Suthers, S.P., Campbell, J.J., Raynlyn, T., Clout, J.M.F., 2006a. Prediction of hydrocyclone performance in iron ore beneficiation using texture classification. Proceedings XXIII International Mineral Processing Congress, Istanbul, pp. 1897–1902.

Donskoi, E., Campbell, J.J., Young, J.M., Raynlyn, T., 2006b. Experimental study of attrition effects in a hematite–goethite iron ore during hydrocycloning. Proceedings XXIII International Mineral Processing Congress, Istanbul, pp. 50–55.

Donskoi, E., Suthers, S.P., Fradd, S.B., Young, J.M., Campbell, J.J., Raynlyn, T.D., Clout, J.M.F., 2007a. Utilization of optical image analysis and automatic texture classification for iron ore particle characterisation. Miner. Eng. 20, 461–471.

Donskoi, E., Campbell, J.J., Young, J.M., Raynlyn, T., Poliakov, A., 2007b. Examination of ultrasonic treatment of iron ore fines using automatic iron ore texture classification. Proceedings, Iron Ore 2007, Fremantle, WA, Australia, pp. 251–257.

Donskoi, E., Suthers, S.P., Campbell, J.J., Raynlyn, T., 2008a. Modelling and optimization of hydrocyclone for iron ore fines beneficiation — using optical image analysis and iron ore texture classification. Int. J. Miner. Process. 87, 106–119.

Donskoi, E., Holmes, R.J., Manuel, J.R., Campbell, J.J., Poliakov, A., Suthers, S.P., Raynlyn, T., 2008b. Utilization of iron ore texture information for prediction of downstream process performance. Proceedings, 9th International Congress for Applied Mineralogy, Brisbane, Australia, pp. 687–693.

Donskoi, E., Poliakov, A., Manuel, J.R., Raynlyn, T.D., 2010a. Advances in optical image analysis and textural classification of iron ore fines. Proceedings, XXV International Mineral Processing Congress — IMPC2010, Brisbane, Australia, pp. 2823–2836.

Donskoi, E., Poliakov, A., Collings, A.F., Bruckard, W.J., 2010b. Ultrasonic treatment of iron ore fines — laboratory study, EP105444, internal CSIRO report.

Farmer, A.D., Collings, A.F., Jameson, G.J., 2000. Effect of ultrasound on surface cleaning of silica particles. Int. J. Miner. Process. 60 (2), 101–113.

Flannigan, D.J., Suslick, K.S., 2005. Plasma formation and temperature measurement during single-bubble cavitation. Nature 434, 52–55.

Franko, J., Klima, M.S., 2002. Application of ultrasonics to enhance wet-drum magnetic separator performance. Miner. Metall. Process. 19 (1), 17–20.

Gogate, P.R., Pandit, A.B., 2001. Hydrodynamic cavitation reactors: a state of the art review. Rev. Chem. Eng. 17 (1), 1–85.

Kelsall, D.F., Restarick, C.J., Stewart, P.S.B., 1974. Technical note on an improved cyclosizing technique. Proc. Australas. Inst. Min. Metall., No 251, pp. 9–10.

Mason, T.J., Lorimer, J.P., 1991. Sonochemistry, Theory, Applications and Uses of Ultrasound in Chemistry. Ellis Horwood Publishers, London.

Pandey, J.C., Sinha, M., Raj, M., 2010. Reducing alumina, silica and phosphorous in iron ore by high intensity power ultrasound. Ironmak. Steelmak. 37 (8), 583–589.

Ross, D., 1976. Mechanics of Underwater Noise Cavitation. Pergamon Press Inc., pp. 203–251 (Chapter 7).

Tao, D., Parekh, B.K., 2000. Enhanced fine coal beneficiation using ultrasonic energy. Miner. Metall. Process. 17 (4), 252–258.

Warren, L.J., 1992. Shear flocculation. In: Laskowski, J.S., Ralston, J. (Eds.), Colloid Chemistry in Mineral Processing. Elsevier, New York, pp. 309–329 (Chapter 10).